

# REPORT 1134

## PHOTOGRAPHIC INVESTIGATION OF COMBUSTION IN A TWO-DIMENSIONAL TRANSPARENT ROCKET ENGINE<sup>1</sup>

By DONALD R. BELLMAN, JACK C. HUMPHREY, and THEODORE MALE

### SUMMARY

Motion pictures at camera speeds up to 3000 frames per second were taken of the combustion of liquid oxygen and a hydrocarbon fuel in a transparent-sided rocket engine. This 100-pound-thrust engine consisted basically of metal contour and injection plates clamped between two plastic sheets. This design provided an essentially two-dimensional engine with a view of the entire combustion chamber. Various injectors, parallel jets and impinging jets, were used in order to study varied types of combustion.

Oxygen-hydrocarbon propellant combinations provided sufficient combustion luminosity to use direct photographic methods. An increase in the number of holes of the parallel-jet injectors tended to increase the uniformity of combustion, but all the injectors showed nonuniformity of combustion. Turbulence projections increased the apparent mixing and circulation of propellants. Variation of ignition delay, apparently from improper mixing, caused starting explosions, midrun explosions, and other short-duration transient phenomena. Both low- and high-frequency oscillations were recorded during the runs, and some of the oscillations corresponded to the resonant frequencies of the chamber. Photographic measurements of gas velocities provided data from which chamber combustion temperatures could be calculated. Patterns in the plastic windows provided additional information regarding gas-flow paths and qualitative indications of temperature variations at the walls.

### INTRODUCTION

Rocket combustion involves a large heat release per unit volume, and the achievement of efficient, steady combustion with a minimum heat loss depends upon carefully designed injector and combustion-chamber configurations. Such designs are best devised on the basis of a knowledge of injector characteristics and combustion gas-flow patterns during transient and steady-state operations within the actual rocket engine. High-speed, motion-picture photography should provide a comprehensive view of flow patterns and time-space data that would be difficult to obtain by other methods. In 1947, a technique was originated at the NACA Lewis laboratory to investigate this supposition in a photographic study of rocket combustion. The technique involves the use of a two-dimensional engine with transparent plastic windows and has three principal advantages: The combustion chamber may be fabricated in uniform thickness; large windows allow the entire chamber to be photographed; and the low-melting material used as windows cannot become luminous and obscure the combustion pattern.

This technique subsequently stimulated photographic research along similar lines (ref. 1) at other laboratories, as well as at the Lewis laboratory. Slit photography, in which a continuous strip camera is used, has also yielded valuable

information about rocket combustion processes (refs. 2 and 3).

The summary presented herein of the photographic-technique research conducted at the Lewis laboratory during 1947-50 includes: (1) a description of the photographic technique; (2) an evaluation of the combustion photographs resulting from the use of three types of injector configuration; and (3) an analysis of some combustion irregularities, such as irregular starts, combustion oscillations, and explosions. Combustion patterns of eight injectors were observed in a 100-pound-thrust, two-dimensional engine in which liquid oxygen and hydrocarbons were used as propellants. Motion pictures of the combustion were taken at camera speeds up to 3000 frames per second. The most important photographs or photographic sequences illustrating the observed phenomena are included in this report. Results of this study are most favorably observed, however, by projection of the film.

### APPARATUS AND PROCEDURE

**Engines.**—Two essentially two-dimensional engines were used in the investigation; the engines differed only in that the first had a transparent-sided nozzle and the second a copper nozzle (see fig. 1). The copper nozzle was used because very rapid erosion of the window in the nozzle of the first engine lowered the chamber pressure and changed the flow in the nozzle.

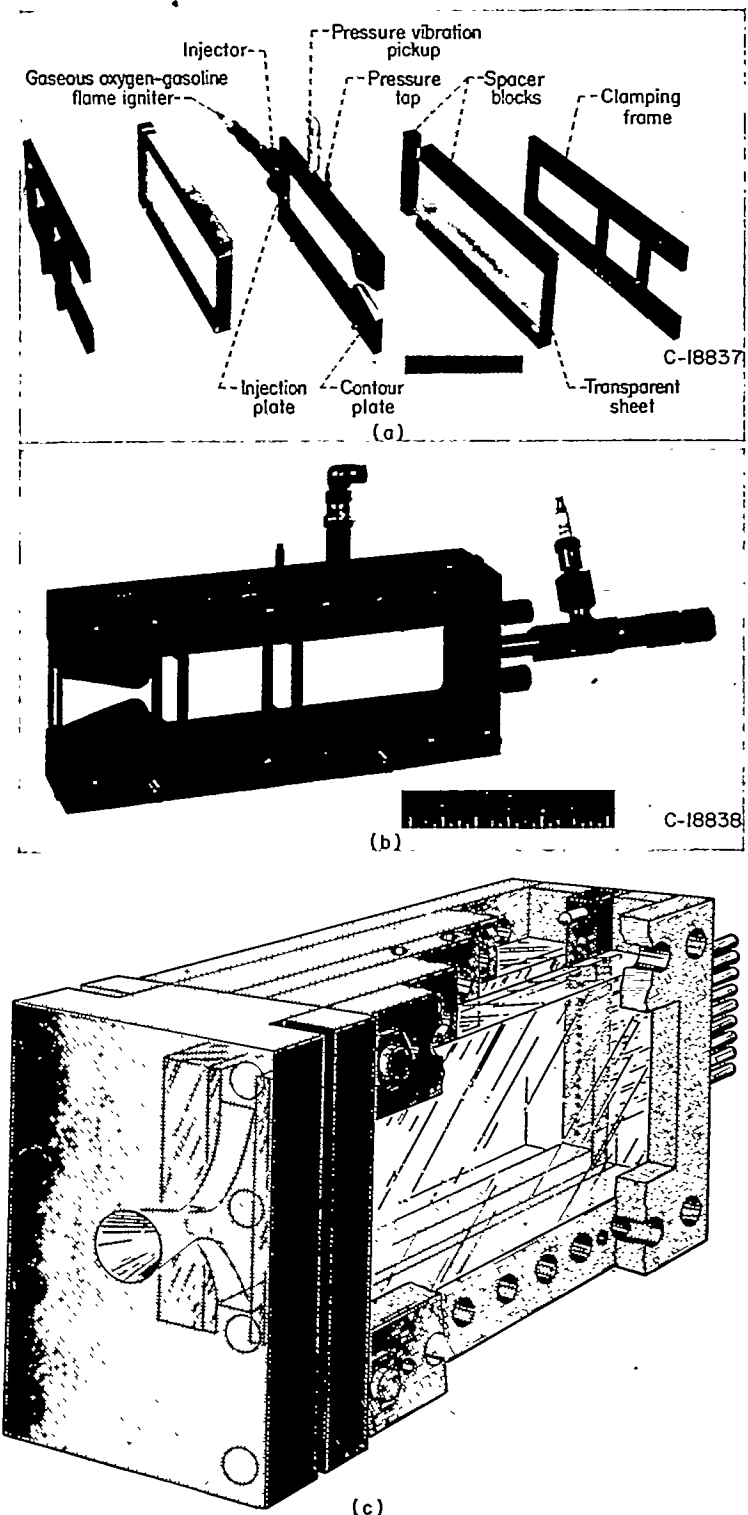
Both engines consisted of contour plates and an injection plate with sheets of transparent material held to both sides of each contour plate by means of suitable spacer blocks and clamping frames. The copper contour plates were chromium plated on the inner surface to reduce erosion by the combustion gases. The transparent sides were polymethylmethacrylate, a transparent plastic that has excellent resistance to thermal shock. The low melting point of the plastic prevented the walls from becoming luminous and thereby obscuring the combustion pattern. The low melting point of the plastic, however, limited the useful duration of a run to a few seconds.

Each side of the rocket consisted of a replaceable inner sheet of  $\frac{1}{4}$ -inch-thick plastic backed by a  $\frac{1}{4}$ -inch-thick supporting sheet of plastic to withstand the combustion pressures. The transparent sheets were sealed to the contour plates with asbestos sheet packing.

The combustion chamber including the nozzle had a uniform thickness of  $\frac{1}{2}$  inch and was designed to produce 100 pounds of thrust with a combustion-chamber pressure of 300 pounds per square inch absolute. The characteristic length (combustion-chamber volume divided by throat area) was about 60 inches. The rocket engine was mounted at a downward angle of  $45^\circ$  to prevent the accumulation of propellants in the chamber in the event of an ignition failure.

<sup>1</sup> Supersedes NACA RM E8F01, "Photographic Study of Combustion in a Rocket Engine, Injection," by Donald R. Bellman and Jack C. Humphrey, 1948.

I—Variation in Combustion of Liquid Oxygen and Gasoline with Seven Methods of Propellant



(a) View of unassembled engine showing transparent nozzle contour plate equipped with single impinging jets.

(b) View of assembled engine showing transparent nozzle contour plate equipped with single impinging jets.

(c) Cutaway view of engine with solid-copper nozzle and equipped with 16-parallel-jet injector.

FIGURE 1.—Transparent-sided rocket engine.

A combustion pressure tap and a pressure vibration pickup were installed through one of the contour plates at about the midpoint of the combustion chamber.

The eight injectors are diagrammatically shown in figures 2 and 3. These may be classed as impinging jets, impinging

jets with turbulence projections, and parallel jets (shower-head). The propellants were ignited either by a gaseous oxygen-alcohol flame, which in turn was ignited by a spark plug, or by a gunpowder squib which was fired into the chamber. For runs 1 to 12, the igniter was located at the center of the injector; for runs 13 to 15, the igniter was mounted perpendicular to the motor axis and  $2\frac{1}{4}$  inches downstream of the injector.

**Propellant systems.**—A schematic diagram of the propellant system used with the first engine in runs 1 to 12 is shown in figure 4. The gasoline tank II was pressurized to 20 pounds per square inch by nitrogen from regulator FF in order to minimize cavitation in the inlet to the pumps. From the tank, the gasoline flowed through rotameter O to two, four-cylinder, positive-displacement pumps DD, which were coupled to a single motor EE. The eight pumping strokes were uniformly staggered to produce a minimum flow variation. From the pump, the gasoline passed through a series of hydraulic resistances BB to eliminate pulsations. The gasoline then flowed either through propellant control valve Z and into combustion chamber V or through relief valve CC and back into the supply tank. During a run, a pressure of about 400 pounds per square inch was required to send the fuel into the combustion chamber, and the relief valve was set at a pressure of 900 pounds per square inch so that no fuel was bypassed when propellant control valve Z was open.

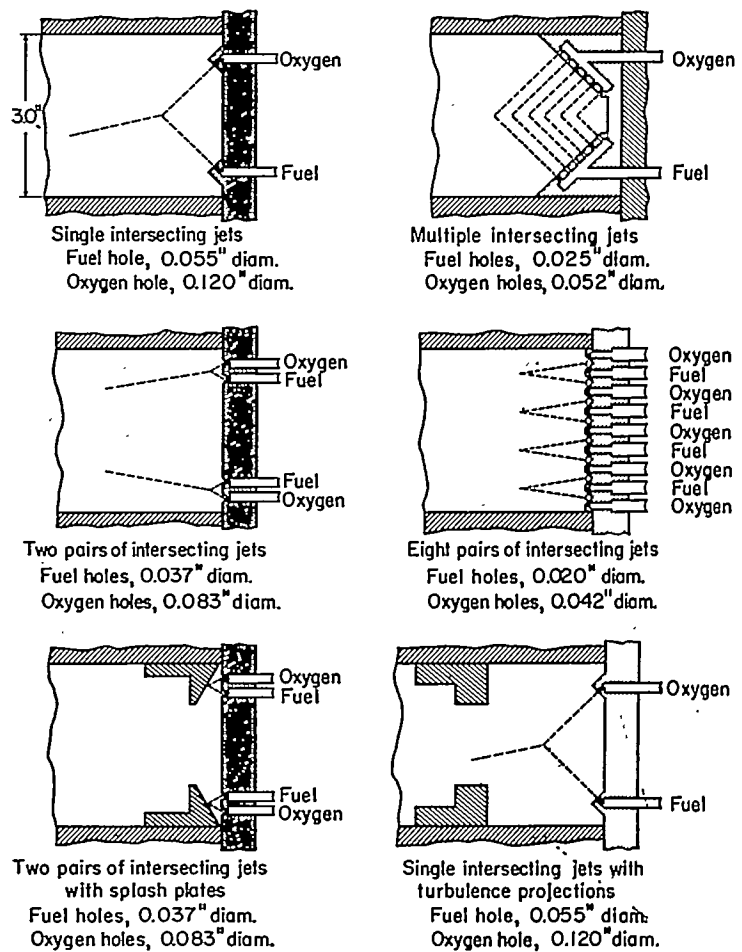


FIGURE 2.—Schematic views of impinging-jet injectors used with two-dimensional, transparent-sided rocket engine.

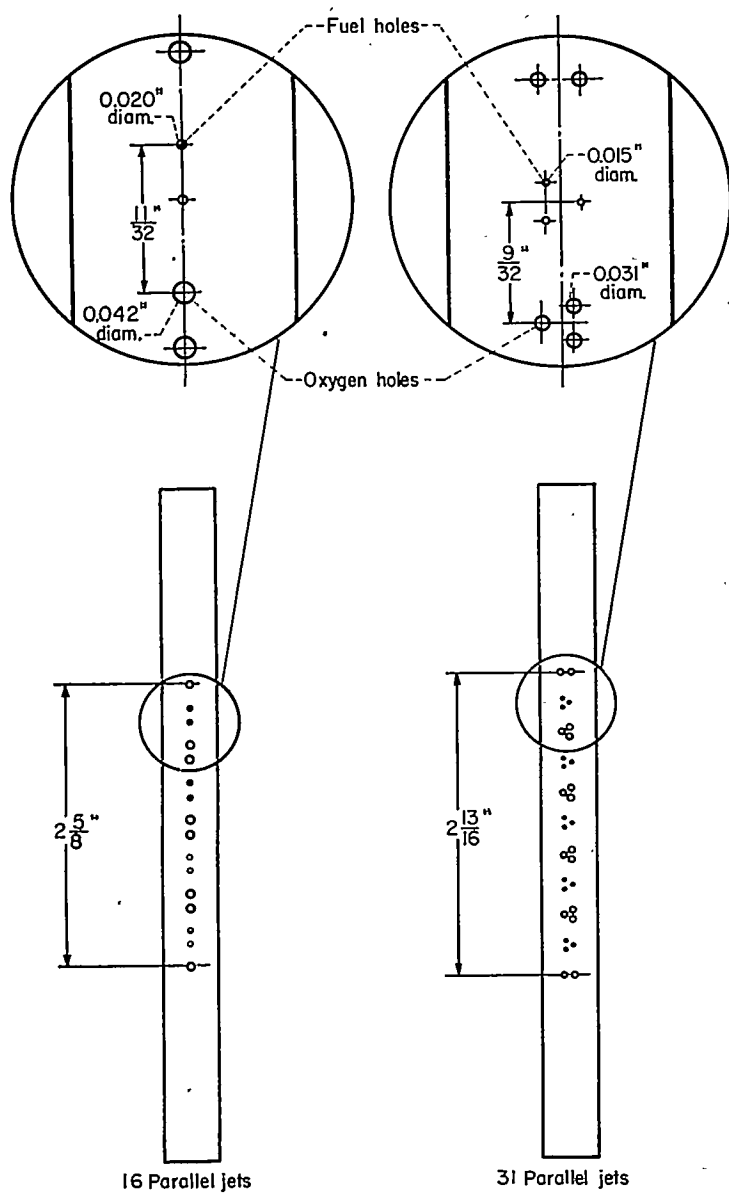


FIGURE 3.—Front view of parallel-jet injectors used with two-dimensional, transparent-sided rocket engine.

The liquid oxygen was stored in a 4-gallon, stainless-steel tank L located close to the combustion chamber. The tank was pressurized to 400 pounds per square inch by means of gaseous oxygen from pressure-reducing valves A and B. From the tank, the liquid oxygen flowed through a vane-type flowmeter T and propellant control valve X to combustion chamber V.

In order to stop the combustion quickly after each run, flushing the liquid-oxygen line with nitrogen was necessary. This flushing was accomplished by pressurizing tank AA with nitrogen during the run by means of three-way solenoid valve F. At the conclusion of each run, the three-way solenoid valve sent the contents of tank AA into the liquid-oxygen line close to the injector, which forced any oxygen remaining in the line out through valve U.

In the portion of this investigation with the engine of figure 1 (c) (runs 13 to 15), a modified system was used. The fuel flow was maintained by means of a gear pump driven at a constant predetermined speed; the flow rate was measured with a rotameter in the pump suction line. Before each

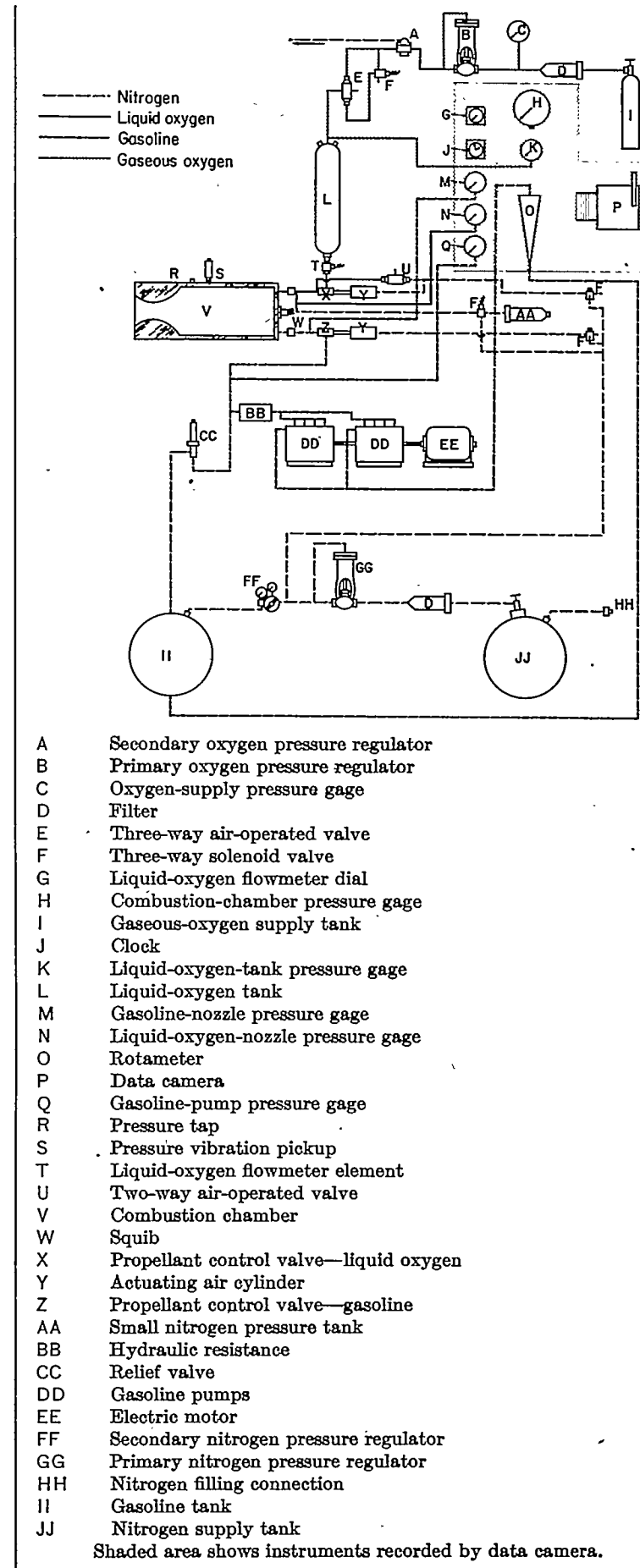


FIGURE 4.—Diagrammatic sketch of propellant and control system for transparent-sided rocket engine.

run, full fuel flow was established and circulated back to the supply tank through a high-pressure relief valve.

The principal difference between this system and the gasoline-oxygen system involved the use of a positive-displacement pump that maintained a constant liquid-oxygen flow over a wide variation of injection pressure. The pump consisted of a cylinder having sufficient volume to hold all the liquid oxygen required for about 5 seconds of operation at the 100-pound-thrust level. A standard hydraulic piston actuated a second piston to force the oxygen from the cylinder, which was kept in a large Dewar flask containing liquid nitrogen. A commercial variable-delivery hydraulic pump maintained the hydraulic pressure to the actuator. Liquid-oxygen flow was determined by measuring the time displacement of the calibrated cylinder.

**Instrumentation.**—Thrust and chamber pressure of the engines were measured in addition to flow rates. Thrust was determined by using a bar spring equipped with strain gages connected in a bridge circuit to a self-balancing recording potentiometer. Chamber pressure was measured by photographing a Bourdon tube gage three times per second; the rate of change of pressure was measured by an engine knock indicator of the magnetostriction type, which was connected to an oscilloscope, and recorded by a moving-film camera. Other auxiliary measurements made are shown in figure 4.

The camera for studying combustion patterns was a 16-millimeter commercial motion-picture camera having a maximum speed of 3000 frames per second; an electronic-wave generator with a constant frequency of 1000 cycles per second marked the film every 1/1000 second.

#### OPERATING CONDITIONS AND PROCEDURE

Commercial liquid oxygen and 62-octane unleaded gasoline (runs 1 to 12) or oxygen and heptane (runs 13 to 15) were used. For a combustion-chamber pressure of 300 pounds per square inch absolute, the theoretical performance of oxygen with these fuels is as follows:

	Gasoline	Heptane
Maximum specific impulse for equilibrium expansion, lb-sec/lb...	261	263
Oxidant-fuel weight ratio for maximum specific impulse.....	2.4	2.4
Combustion temperature for maximum specific impulse, °R.....	6270	6180

Before a run, the flows were preset in an attempt to obtain an oxidant-fuel weight ratio of 2.4. All the firing operations, including shutdown, were automatically performed upon closing of a single switch. The following schedule was used: Liquid-oxygen flow was started and a 15-second delay allowed the oxygen lines and injector to cool and reach the proper flow rates; at 15 seconds, the high-speed camera was started and the squib ignited; at 16 seconds, the fuel was admitted and ignition took place. As soon as all the film in the camera was exposed, the propellant flow was stopped and the liquid-oxygen line was flushed with nitrogen.

Since the camera film length allowed an exposure time of less than 3 seconds, the run was scheduled to last about 1½ seconds. After each run, the inner sheets of the transparent sides and the squib were replaced.

#### GENERAL COMBUSTION PHENOMENA

The combustion-phenomena discussion is subsequently broken down into the various injector configurations, plastic-window patterns, performance, and temperature calculations. In a later section, selected photographs show irregular combustion phenomena of starting characteristics, explosions, and oscillations.

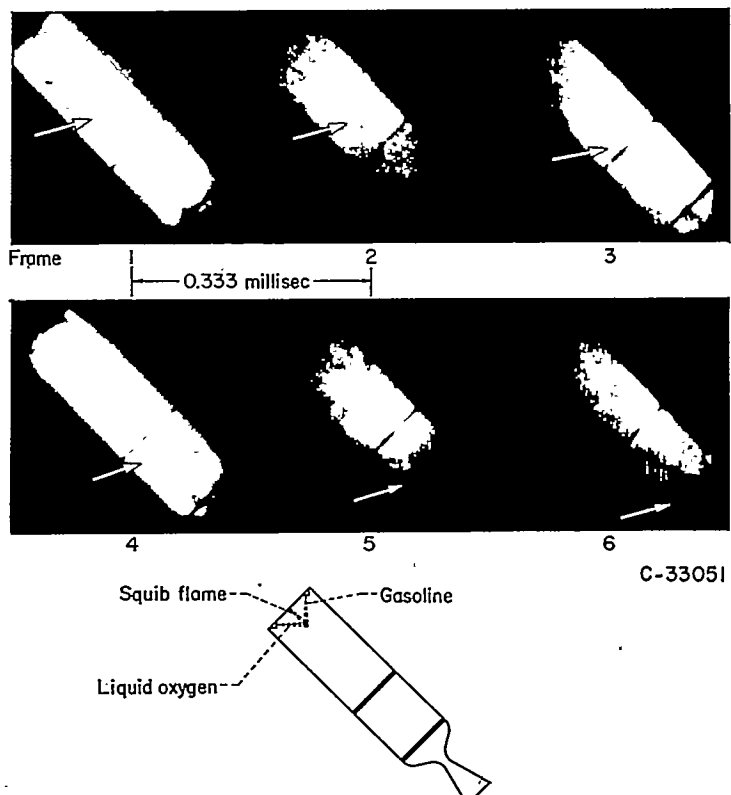
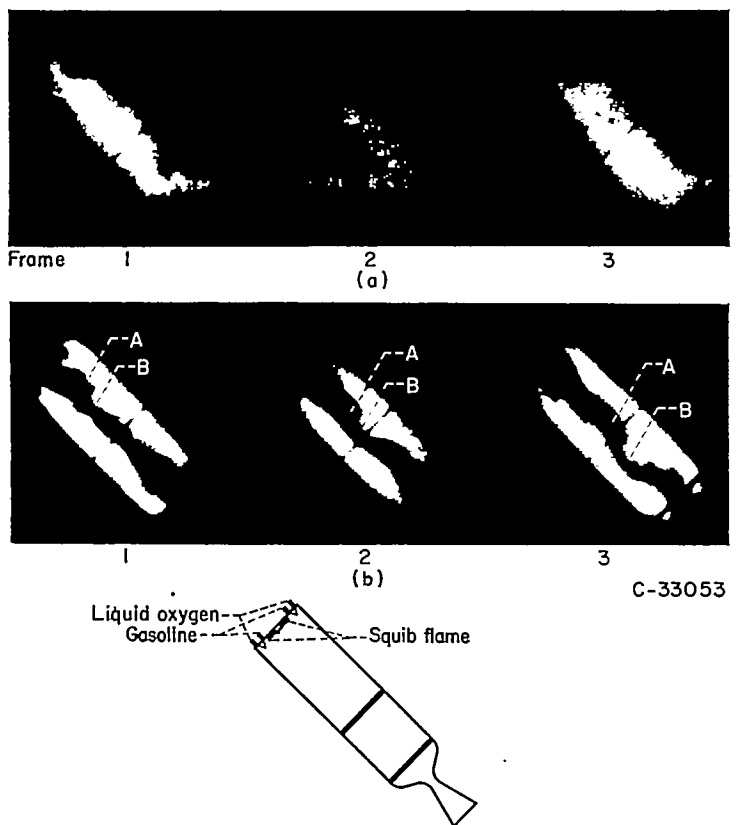


FIGURE 5.—Combustion of liquid oxygen and gasoline in transparent-sided rocket engine with single intersecting jets, and with motion of nonluminous pocket (arrows) shown. Run 1; camera speed, 3000 frames per second; thrust, 75 pounds.

#### COMBUSTION PATTERNS WITH VARIOUS INJECTORS

**Intersecting jets.**—Combustion with four combinations of intersecting-jet injectors is shown in figures 5 to 9. All the figures show some nonuniform light emission, and pockets of nonluminous gases appeared randomly through all the photographs. Some of the pockets retained their identity as they flowed through the chamber, as indicated by the arrows of figure 5. With two widely spaced pairs of intersecting jets, the resulting photographs often show, as in figure 6 (b), a dark region in the vicinity of the fuel jets and a center core of nonluminous gas that moved through the chamber as an undulating core. It might appear at first inspection that lateral movement existed to cause the undulation. However, closer inspection of the original photographs shows that dark areas arose in the injector fuel area and the luminous lobes emerged from the side areas; but the dark area, A in figure 6 (b), and the luminous areas, B in figure 6 (b), passed through the chamber almost undeviated from the longitudinal path originating near the injector. The wavy core was apparently made up of pockets of non-reacting propellant mixtures that were displaced laterally and were so close together that they were joined.



(a) Run 11; camera speed, 2380 frames per second; thrust, 73 pounds.  
 (b) Run 12; camera speed, 2780 frames per second; thrust, 65 pounds.

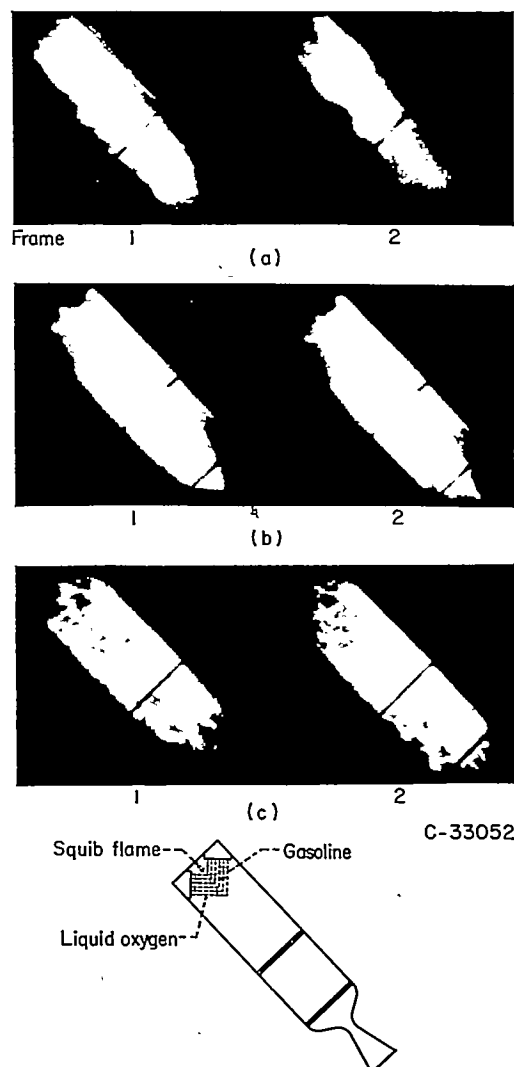
FIGURE 6.—Combustion of liquid oxygen and gasoline in transparent-sided rocket engine with two sets of single intersecting jets.

The luminous gas outside the engine (figs. 5 and 7) was a reflection of combustion light by external oxygen vapor. Figure 8 shows two pairs of intersecting jets with projections mounted as splash plates; areas of nonluminous gas existed in the injector area, and two dark streaks often appeared to stream from the tips of the splash plates.

**Intersecting jets with turbulence projections.**—Photographs of intersecting jets with the turbulence projections mounted about  $3\frac{1}{4}$  inches downstream of the injector faces are shown in figures 10 and 11. The projections created additional turbulence and circulation of propellants and tended to form pockets of nonluminous gases downstream of the projections.

**Parallel jets.**—Combustion with 16 and 31 parallel jets is shown in figures 12 and 13, respectively. Both of these injectors showed a striated pattern of smooth stream flow with varying intensity of luminosity across the stream lines. An increase in the subdivision of the propellant streams tended to increase the uniformity of luminosity.

A major problem of rocket combustion, poor propellant mixing, is illustrated by the 16-parallel-jet injector (fig. 14). The injector was located at the left of the photograph in figure 14 (a) and propellant flow was from left to right and out of the nozzle not shown in the photograph. From the midchamber area to the nozzle, five bright zones A of illumination or apparent combustion are separated by four dark zones B of noncombustion. About halfway between the midchamber area and the injector, zones of intense brightness C alternate with zones of lesser brightness D.



(a) Run 3; camera speed, 2835 frames per second; thrust, 112 pounds.  
 (b) Run 4; camera speed, 2810 frames per second; thrust, 84 pounds.  
 (c) Run 5; camera speed, 2875 frames per second; thrust, 91 pounds.

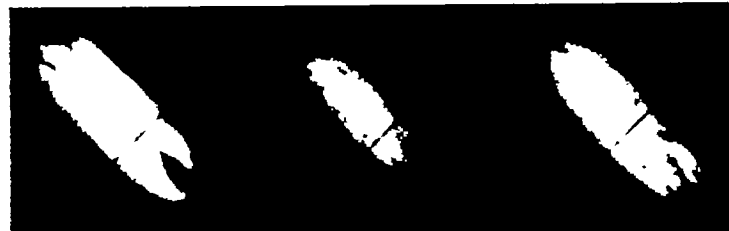
FIGURE 7.—Combustion of liquid oxygen and gasoline in transparent-sided rocket engine with multiple intersecting jets.

The over-all bright area near the injector may be explained as follows: With most liquid sprays, the friction of gases causes small fragments of liquid to peel off the liquid spray and form a mist. It is reasonable to assume that some mist mixing would occur as a result of interaction of the propellant pairs as well as interaction between the two different propellants.

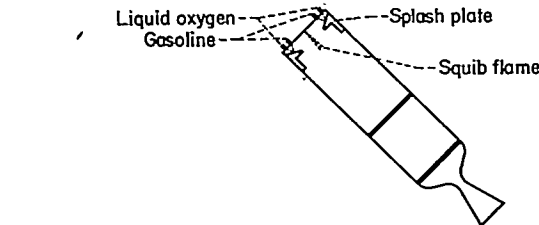
Primary mixing of the propellants would occur as the streams individually expand and finally touch. Run 14 (fig. 12), when examined under motion-picture projection, shows practically no longitudinal turbulence except near the injector and very little lateral turbulence. A possible schematic spray configuration is shown in figure 14 (b), which illustrates how the propellant streams can mix at some station downstream and react. This mixing and reacting cause illumination and exposure of the photographic film as shown by figure 14 (a). The gray regions represent the unburned propellants, and the white regions represent combustion where interaction takes place. The schematic illustration is based upon the actual injector in which there were five oxidant zones and four fuel zones resulting in eight



Frame 1 2 3  
(a)



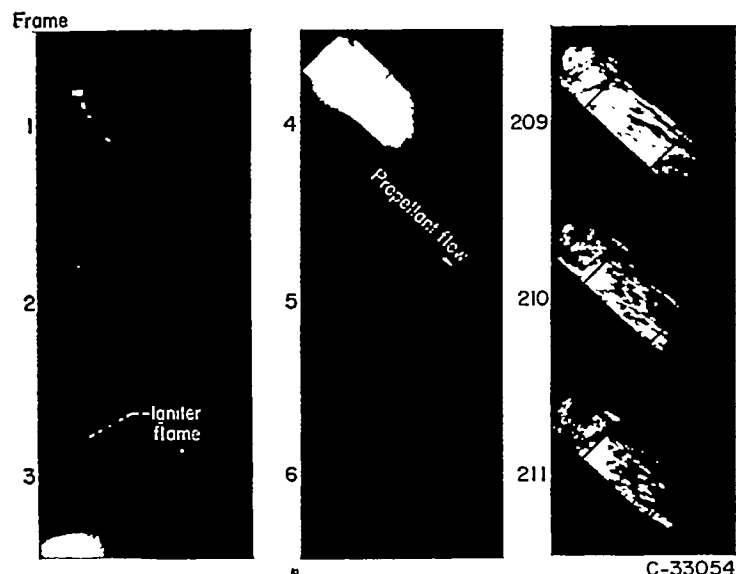
Frame 1 2 3  
(b) C-33055



(a) Run 9; camera speed, 2860 frames per second; thrust, approximately 100 pounds.

(b) Run 10; camera speed, 2940 frames per second; thrust, 115 pounds.

FIGURE 8.—Combustion of liquid oxygen and gasoline in transparent-sided rocket engine with two pairs of intersecting jets with splash plates.



Frame 1 2 3 4 5 6 209 210 211  
C-33054

FIGURE 9.—Start of combustion and steady-state burning of liquid oxygen and gasoline in transparent-sided rocket engine with multiple intersecting jets. Run 13; camera speed at frame 4, 857 frames per second; camera speed at frame 210, 1091 frames per second.

mixing zones. Figure 14 (a) shows eight zones of high intensity, and the high-intensity zones can actually be perceived in the original photographs as close as 1 inch from the injector. The mist and earlier turbulent mixing could cause the apparent blurred brightness near the injector,



Frame 1 2 3  
C-33056

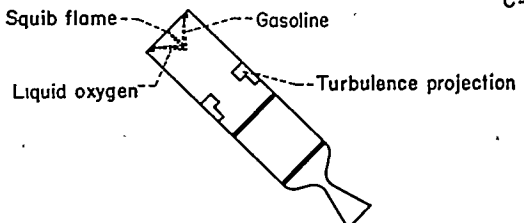
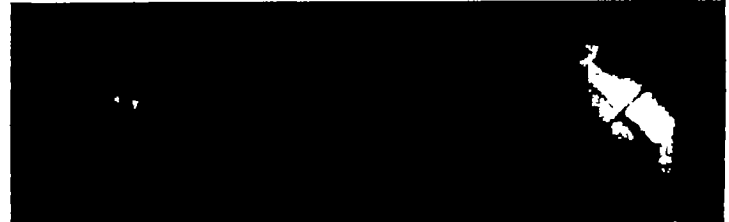


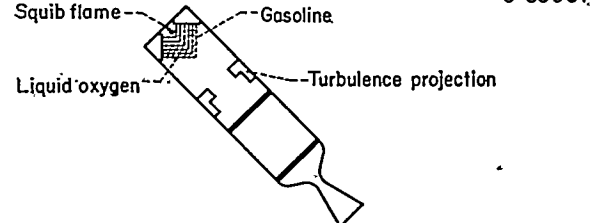
FIGURE 10.—Combustion of liquid oxygen and gasoline in transparent-sided rocket engine with single intersecting jets with turbulence projections. Run 2; camera speed, 3165 frames per second; thrust, 96 pounds.



Frame 1 2 3  
(b)



Frame 1 2 3  
(a) C-33057



(a) Run 7; camera speed, 1935 frames per second; thrust, 113 pounds.

(b) Run 8; camera speed, 2490 frames per second; thrust, 72 pounds.

FIGURE 11.—Combustion of liquid oxygen and gasoline in transparent-sided rocket engine with multiple intersecting jets with turbulence projections.

but the core or main stream of the jets ultimately shows downstream the basic pattern of the injector.

The magnitude of the small-scale lateral turbulence increased as the propellants moved toward the nozzle, but one basic pattern emerged: The number of dark zones corresponded exactly to the number of injector fuel zones and probably were caused by highly concentrated unreacted fuel. Also, the broad zones of combustion had a somewhat indistinct darkened core which probably was highly concen-

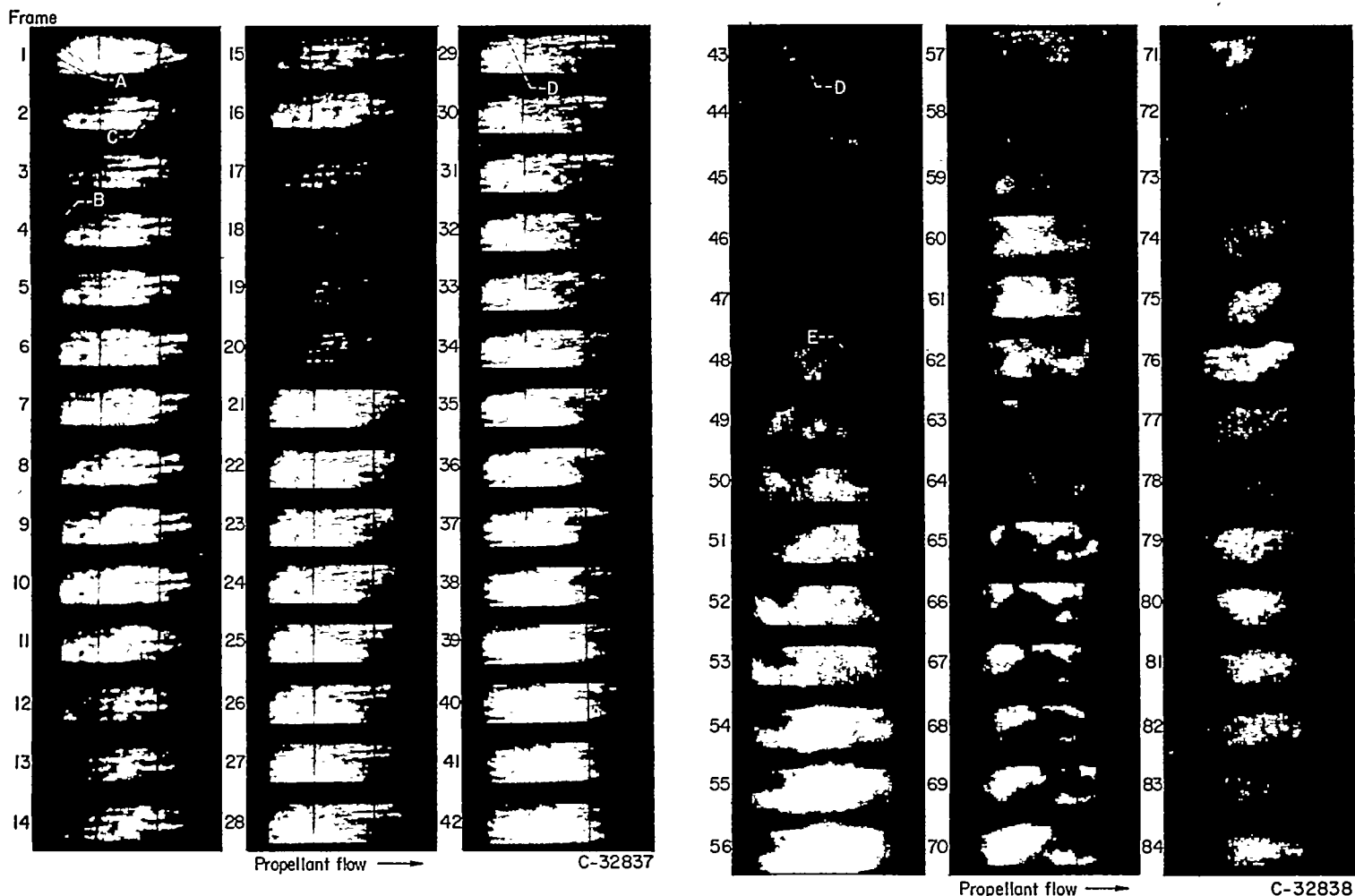


FIGURE 12.—Combustion of liquid oxygen and heptane in transparent-sided rocket engine with 16-parallel-jet injector. Run 14; thrust, approximately 79 pounds; camera speed at frame 1, 2500 frames per second; camera speed at frame 84, 2525 frames per second.

trated unused oxygen. The sides of the bright zones were obvious continuations of the eight high-intensity zones mentioned earlier. Reference 1 also reports that striations occurred in some systems, that the dark areas corresponded to fuel zones, and that the bright areas corresponded to oxidant zones. This over-all appearance leads to the postulation that fuel-rich mixtures of oxygen-hydrocarbons do not burn as well as oxidant-rich mixtures. It is not known what these mixtures were, but it seems reasonable from observation of the smooth streaming flow that the center cores of both the oxidant and the fuel zones were richer than the normal off-stoichiometric mixtures usually considered. The preceding postulation is further substantiated by an explosion, mentioned later in **IRREGULAR COMBUSTION PHENOMENA**, in which an unburned slug appears to come from a fuel zone.

#### BURN PATTERNS IN PLASTIC WINDOWS

Most of the photographs of burn patterns in plastic windows show a great deal of stratification at the nozzle throat. The plastic was burned to a lesser depth behind the dark streaks than behind the bright areas. This effect is shown in figure 15, in which a photograph of the combustion during one of the runs is compared with the plastic window from that run. On the bottom side of the nozzle throat, the

flame burned completely through the  $\frac{1}{4}$ -inch plate and slightly into the backing plate; on the top side, the plastic did not burn through. The combustion photograph shows that the top side, which has the less luminous area, was not burned so deeply. Thus, nonuniform flow through the nozzle with the possibility of asymmetric thrust forces is indicated.

The luminosity of the gases decreased very rapidly as the gases passed into the divergent section of the nozzle probably because of a decrease in both temperature and density. Even though the flame outside the rocket engine appeared very bright to the eye, it was not bright enough to record on the high-speed photographs. Figure 15 further shows that in the divergent section of the nozzle a pattern in which the Mach lines are discernible was burned into the plastic windows.

The plastic windows alone form an interesting record of the run, for they show variations in the injector action by burning to a greater depth in line with some of the propellant streams. If such burning occurs more on one plate than on the other, poor alinement of the propellant streams is indicated. The sides also show some of the flow variations, particularly around the turbulence projections and in the nozzle region. In most cases, the nozzle throats were burned deeper at the edges than in the middle of the plastic surface,

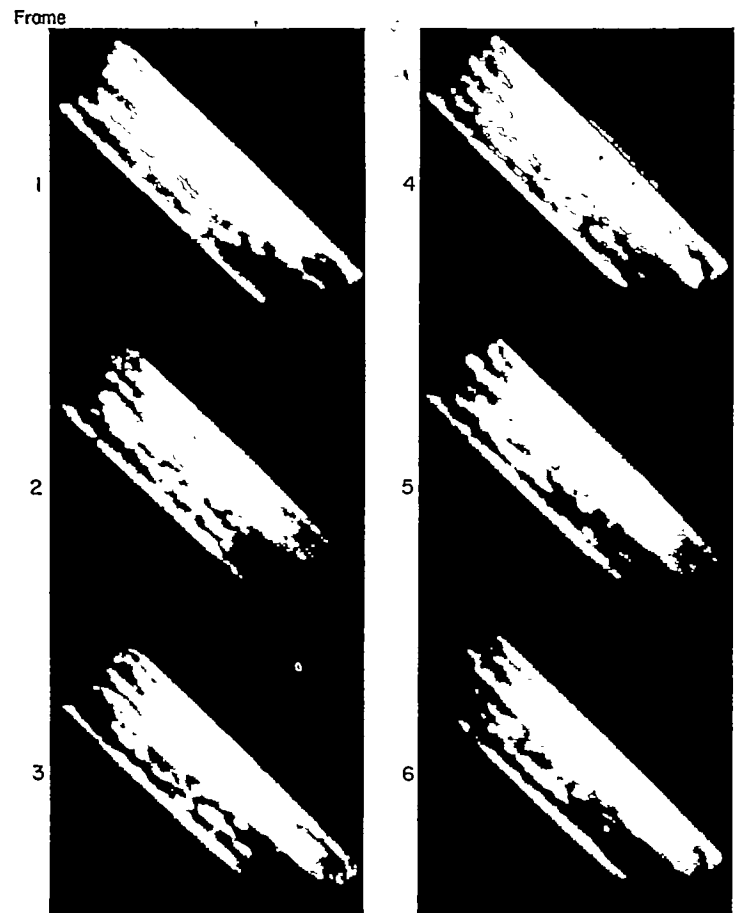


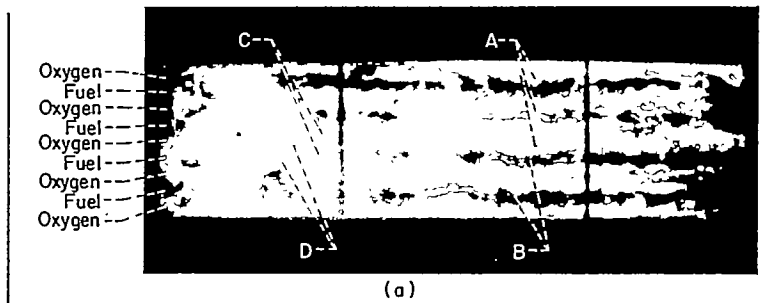
FIGURE 13.—Full chamber view of combustion of liquid oxygen and heptane in transparent-sided rocket engine with 31-parallel-jet injector. Run 15; thrust, 134 pounds; camera speed, 1845 frames per second.

which indicated either higher velocities or higher temperatures at the edges. In the divergent section of the nozzle, the Mach angle can be measured from the pattern formed there and gives an additional check on the calculated conditions. In the runs presented herein, however, conditions varied too greatly from the beginning to the end of the run for such a measurement to have much value.

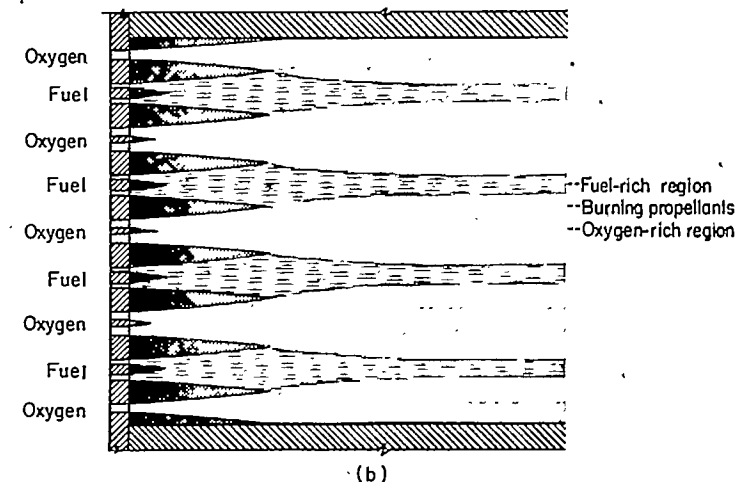
## **PERFORMANCE**

**Thrust measurement.**—It was found that engine performance data could not be measured with sufficient accuracy to make comparisons among the various injector configurations used. The short operating time, the lack of rapid-response instrumentation (except rate of change of pressure), the intermittent recording of chamber pressure and flow, the consumption of plastic during a run (up to 20 percent of the total flow), and the rapid erosion of the throat of the plastic nozzle were all contributing factors in preventing accurate performance measurements. Table I shows approximate performance data for use as a guide in studying the combustion photographs. Since thrust was measured continuously, it was used as a qualitative indication of performance, although this use can be misleading when there are large variations in chamber pressure and flows.

**Temperature calculations.**—For many of the runs, measurement of the velocity of the propellant gases was possible in the combustion chamber from observations of the move-



Propellant  
orifice  
positions



(a) Enlargement of frame from run 14, 63 seconds after start of combustion. Approximately one-tenth actual size of engine window and magnified 10 times from negative.

FIGURE 14.—Schematic illustration of propellant spray configuration showing primary zones of mixing (light areas).

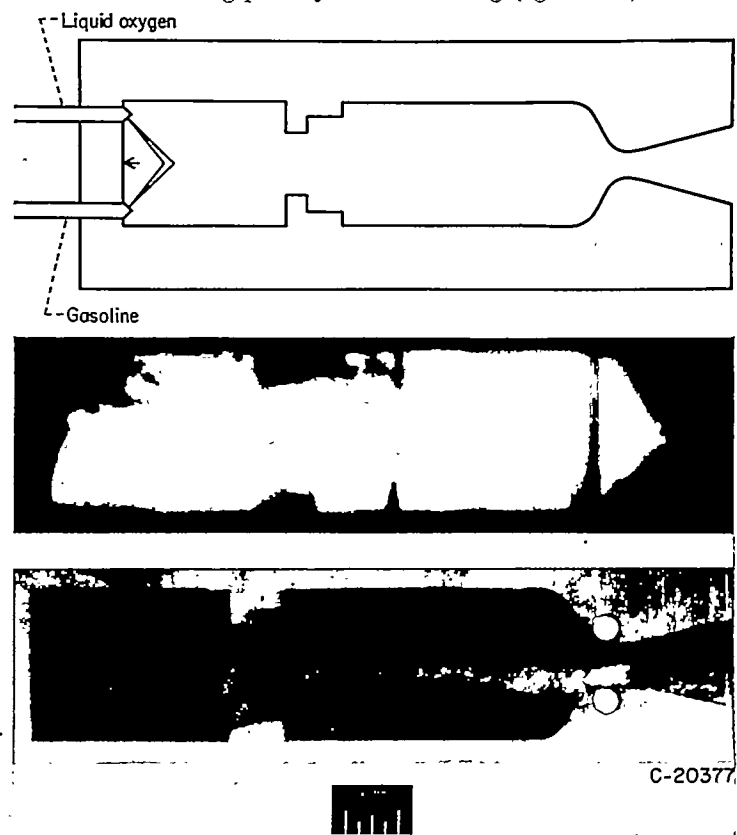


FIGURE 15.—Plastic plate after run of 1.9 seconds and combustion taken through same plate. Run 2.

TABLE I.—APPROXIMATE PERFORMANCE DATA

Run	Injector	Hydrocarbon propellant	Fuel flow, lb/sec	Oxidant flow, lb/sec	Thrust, lb	Combustion-chamber pressure, $P_c$ , lb/sq in. abs
Engine 1 (plastic nozzle)						
1	Single intersecting jets...	Gasoline.....	....	....	75	.....
2	Single intersecting jets with turbulence projections.	Gasoline.....	0.16	0.33	96	180
3	Multiple intersecting jets.	Gasoline.....	0.17	0.60	112	223
4			.17	.34	84	230
5			.17	.35	91	215
6			.16	.45	110	242
7	Multiple intersecting jets with turbulence projections.	Gasoline.....	0.18	0.35	113	.....
8			.18	.23	72	173
9	2 Pairs of intersecting jets with splash plates.	Gasoline.....	0.18	0.24	100	196
10			.18	.42	115	246
11	2 Pairs of intersecting jets.	Gasoline.....	0.18	0.24	73	176
12			.16	.21	65	164
Engine 2 (copper nozzle)						
13	8 Pairs of intersecting jets.	Gasoline.....	0.15	0.39	90	165
14	16 Parallel jets.....	Heptane.....	0.14	0.32	79	>200
15	31 Parallel jets.....	Heptane.....	0.16	0.34	>100	>300

ment of a nonluminous pocket. With the use of this value, together with measured values for combustion-chamber pressure, weight flow, and area in accordance with the following equation, the ratio of the combustion temperature to the molecular weight of the products  $T_c/m$  can be determined:

$$\frac{T_c}{m} = \frac{V_c P_c A_c}{WR} \quad (1)$$

where

- $T_c$  combustion-chamber temperature
- $m$  average molecular weight of combustion gases
- $V_c$  gas velocity in combustion chamber
- $P_c$  combustion-chamber pressure
- $A_c$  combustion-chamber cross-sectional area
- $W$  total propellant weight flow
- $R$  universal gas constant

In most of these experiments, the cross-sectional area and the combustion-chamber pressure continually changed and there was insufficient timing correlation to determine values for the pressure and the area at the exact time for which the velocity was measured. These measurement uncertainties allow only an approximate measurement of  $T_c/m$  by the use of equation (1). The ratio  $T_c/m$  can be determined from other measured quantities; thus

$$\frac{T_c}{m} = \left( V_c \frac{A_c}{A_t} \right)^2 \left[ \frac{M^2(\gamma - 1) + 2}{\gamma + 1} \right]^{-\frac{1}{\gamma - 1}} \frac{1}{\gamma g R} \quad (2)$$

where

- $A_t$  nozzle-throat area
- $M$  combustion-chamber Mach number
- $\gamma$  ratio of specific heats
- $g$  acceleration due to gravity

Equation (2) can be derived from Bernoulli's equation by assuming an isentropic process. The ratio of specific heats cannot be experimentally measured, but the use of the

theoretical value of the ratio of specific heats introduces only a small error. For most rocket engines, the effect of combustion-chamber Mach number is so small that it can be neglected. In the first 12 experiments reported, the nozzle-throat area varied greatly during the runs, and consequently the use of equation (2) to determine  $T_c/m$  is also subject to measurement uncertainties. The following table presents the ratio of the measured values of  $T_c/m$  as determined by the use of equations (1) and (2) to the theoretical values of  $T_c/m$ :

Run	Injector system	Theoretical $T_c/m$	Measured $T_c/m$ / Theoretical $T_c/m$	
			Equation (1)	Equation (2)
5	Multiple intersecting jets without turbulence projections.....	250	0.48	0.39
11	Two pairs of intersecting jets with splash plates.....	260	0.71	0.65
15	16 Parallel jets.....	287	0.59	0.58
16	31 Parallel jets.....	257	0.72	0.48

The areas used for the values shown in the table were those for the start of the run for the transparent nozzle (runs 4 and 10). Other values used were taken at the maximum combustion-chamber pressure. During each run with the transparent nozzle, the nozzle-throat area changed by a factor of 2; hence the measurement uncertainties for the variables of equation (1) were probably less than those for equation (2). By the use of equation (1), the results show that the measured  $T_c/m$  varies from about 40 to about 70 percent of the theoretical  $T_c/m$ .

## IRREGULAR COMBUSTION PHENOMENA

### STARTING CHARACTERISTICS

Some starts were smooth; that is, the combustion spread in a steady manner throughout the chamber. Other runs were erratic; at the start of these runs, a small flame appeared in the vicinity of the intersection of the propellant jets. This flame swelled and diminished in an irregular and uneven manner during the time it was extending to fill the combustion chamber. In many runs, about  $\frac{1}{2}$  second was required for the flame to fill the entire chamber and to become relatively stable. Some times the start consisted of a series of explosions, as shown by the sequence of photographs in figure 16. Explosive starts frequently caused bursting of the windows; this same phenomenon could damage metal chambers.

### EXPLOSIONS

Starting explosions can exist in a mild form, as illustrated in figure 16, or as more disastrous starts, which are difficult to record and to evaluate. In figure 16 the burning appears to be normally smooth during the first cycle, which peaks at frame 5. However, the burning in the second and third cycles, which peak at frames 27 and 51, respectively, was explosive. The spatial luminosity change between frames 25 and 26 is faster than the movement of propellants through the same space (normally in the range of 100 to 300 ft/sec). Therefore, it seems reasonable to conclude that an unburned mixture was conditioned to become explosive and that some unrecorded disturbances triggered the combustion

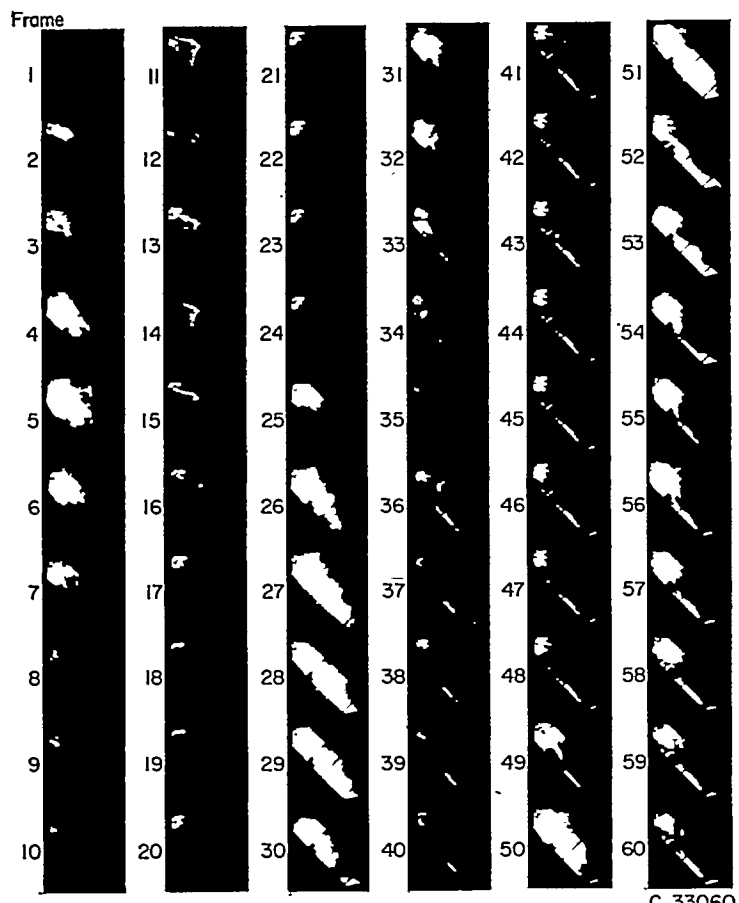


FIGURE 16.—Starting explosions of liquid oxygen and gasoline in transparent-sided rocket engine with multiple intersecting jets with turbulence projections. Run 8; camera speed at frame 1, 602 frames per second; camera speed at frame 60, 695 frames per second.

almost simultaneously throughout all parts of the chamber or triggered the mixture by a wave compression.

Another sequence in which the start was explosive is shown in figure 9, frames 1 to 6. Since only the igniter flame appears in frame 3 and the entire chamber is luminous by frame 5, no upper limit of spatial velocity can be computed; but a flame velocity of about 500 feet per second or greater is indicated because the flame fills the first 7 inches of the chamber of frame 4.

Explosions from previously mentioned improper mixing may occur during the middle of a run, as shown by figure 12. Projection of the sequence showed that the start was cyclic but that smooth streaming combustion existed by the first frame of figure 12. Four dark areas, A in frame 1, project into the chamber area and pulsate longitudinally, sometimes becoming quite small and other times quite extensive. One or both of the top dark areas indicate malfunctioning of the injector, as evidenced by propellant circulation in that area and shown by B in frame 4. Momentary malfunction may or may not be serious; for example, a slug of apparently unburned propellant passed harmlessly through the chamber (indicated in frame 2 of fig. 12 by C).

Soon afterwards another slug of unburned propellant started through the chamber as shown, for example, by D in frames 29 and 43, but this slug exploded when it reached position E in frame 48. Apparently, the second slug had

sufficient ignition delay to become explosive. The combustion mechanism or rate appeared to be changed, as evidenced by the increased luminosity. The injector flow was disturbed by the explosion but quickly reestablished itself (frames 61 to 63); combustion rapidly followed the reestablishment of the injector flow, the explosion gases were swept from the chamber, and the system appeared to be normal by frame 84, except for occasional slugs of unburned propellant that did not explode (typical of that shown by F in frame 78). The sequence showing the midrun explosion indicates a condition that also may cause destructive damage to engines.

From the photographs it appears that the variation of ignition lag from improper mixing indicates a propellant mixture ratio that can cause starting explosions, midrun explosions, and other transient phenomena.

#### COMBUSTION OSCILLATIONS

Low-frequency oscillations, commonly known as "chugging," are illustrated in the sequence of figure 17. The phenomenon of chugging was first encountered and perceived through the technique of transparent chamber photography. Figure 17 shows  $2\frac{1}{4}$  cycles of chugging with a frequency of approximately 98 cycles per second. Another sequence, not

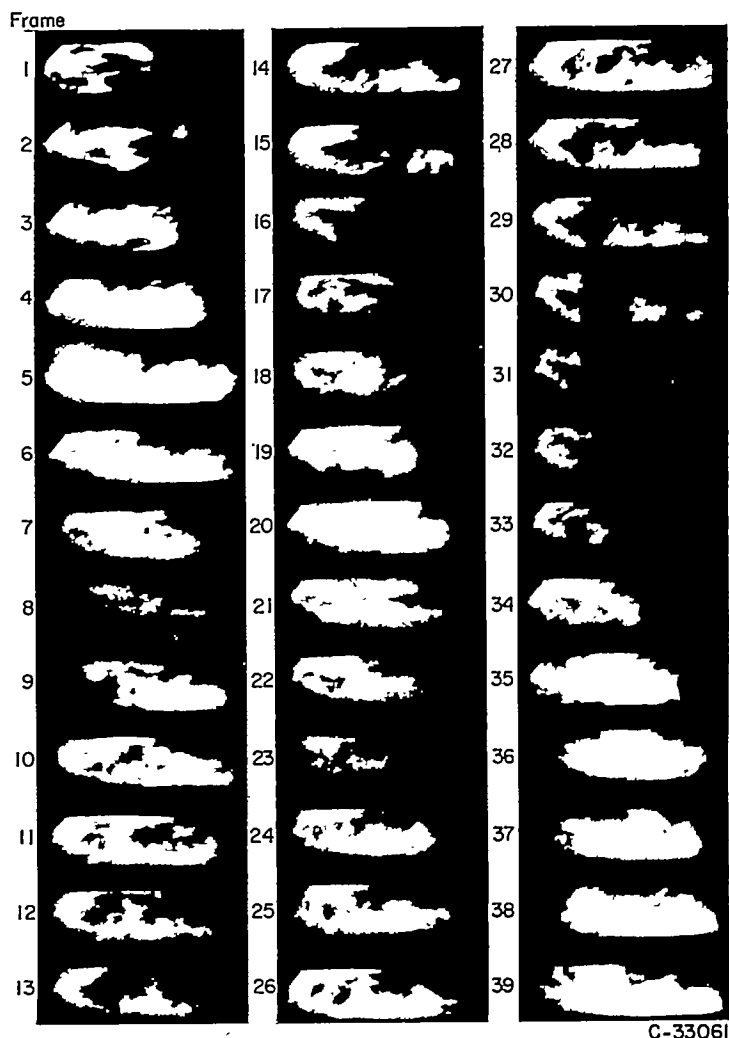


FIGURE 17.—Low-frequency oscillations or "chugging." Chugging frequency, 98 cycles per second; camera speed, 1500 frames per second.

illustrated, was analyzed and found to give a frequency of 103 cycles per second. Chugging is characterized by arrested flow within the chamber and sometimes by flow reversal. Analysis of propellant flows and chamber combustion parameters (ref. 4) has revealed a logical explanation of chugging. The analysis shows chugging to be an out-of-phase coupling between the fluid flow of the propellant feed system and the combustion process in the rocket chamber. Low propellant pressure drop across the injector aggravates chugging, which usually can be alleviated by use of an injector design that incorporates the use of higher pressure drop. During the start of many of the runs, a distinct oscillation of 100 to 300 cycles per second existed. This oscillation corresponded to a brightening and dimming throughout the entire combustion chamber, as illustrated in figure 14.

High-frequency oscillations have also been encountered. When  $T_c/m$  is known, computation of the speed of sound through the combustion gases and thus of the various natural frequencies of the chamber is possible. By use of an average value of  $T_c/m$  as obtained by means of equation (1) and a theoretical value for the ratio of specific heats, the following

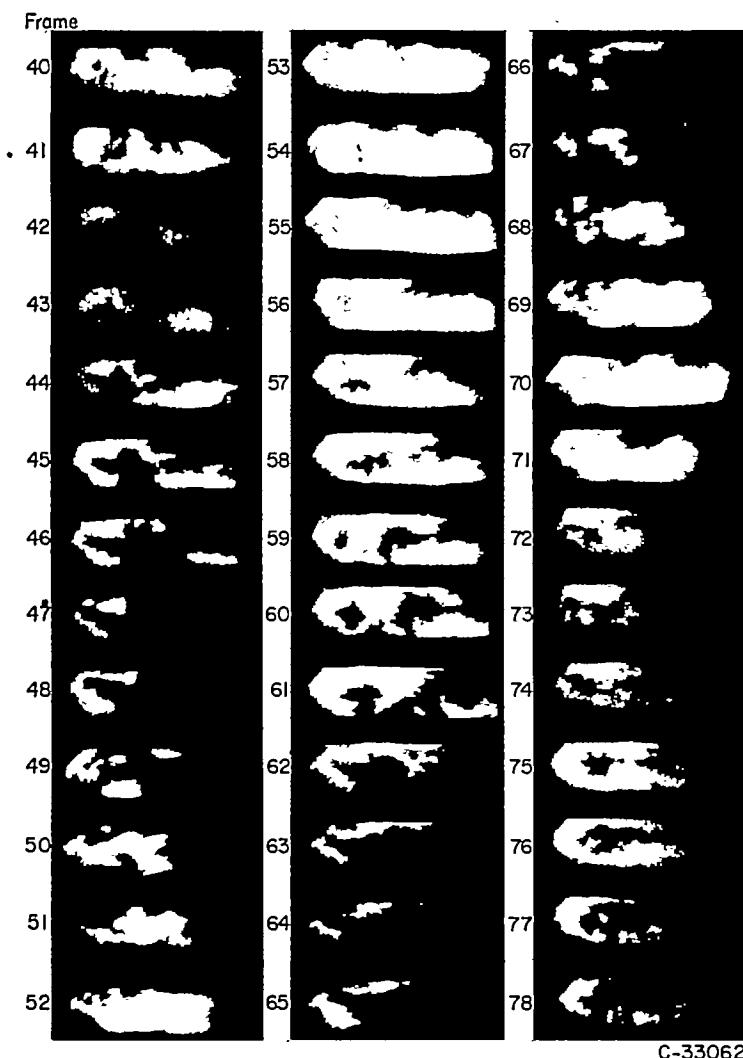
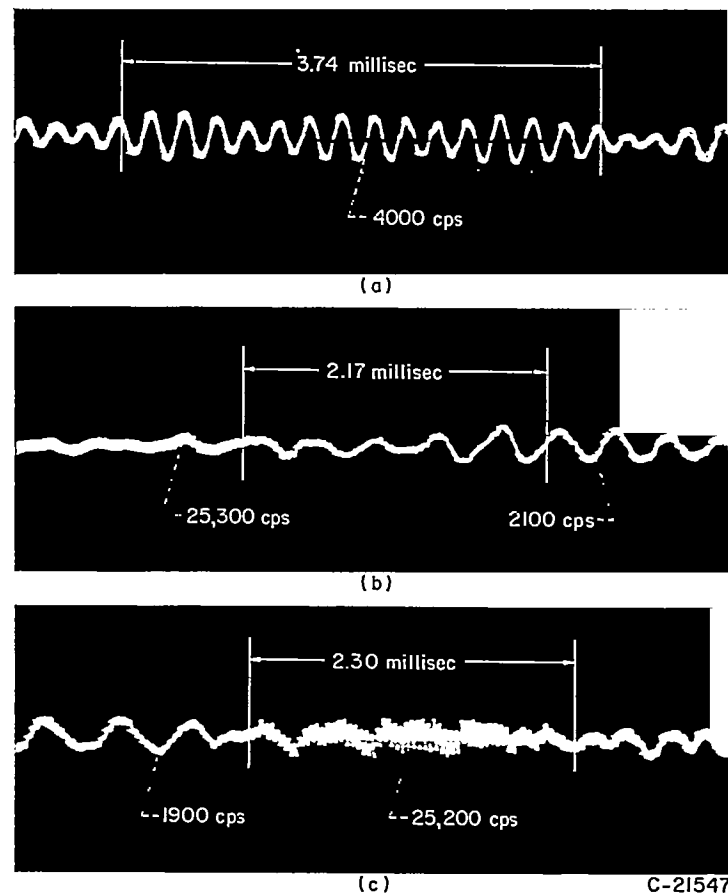


FIGURE 17—Concluded. Low-frequency oscillations or "chugging." Chugging frequency, 98 cycles per second; camera speed, 1500 frames per second.



(a) Before start of run.  
 (b) After start of run.  
 (c) Near end of run.

FIGURE 18.—Combustion-chamber-pressure oscillation records with magnetostriiction-type pressure pickup. Run 6.

values were determined for the natural frequencies of the combustion chamber:

Dimension	Frequency, cps
Length.....	1800
Width.....	6000
Thickness.....	33,000

In the combustion-chamber-pressure oscillation records, two vibration frequencies were prominent throughout the runs: one at approximately 1900 cycles per second and the other at approximately 25,000 cycles per second. These oscillations, therefore, approximately correspond to the natural frequencies for the length and thickness of the chamber. Samples of the various oscillation records are shown in figure 18. Occasionally a frequency of about 4000 cycles per second was recorded, and this frequency was found to be the natural frequency of the thrust stand.

#### SUMMARY OF RESULTS

A technique was developed that used high-speed, motion-picture photography to study combustion in a 100-pound-thrust, transparent-sided, two-dimensional rocket engine. Oxygen and either gasoline or heptane were introduced into the chamber through a variety of injectors, and motion pictures of the burning process along with simultaneous recordings of operational and oscillatory data were taken.

The following results were obtained:

1. All the injectors showed nonuniformity of combustion.
2. Turbulence projections used with the injectors increased the apparent mixing and circulation of propellants.
3. An increase in the number of holes of the parallel-jet injectors tended to increase the uniformity of combustion.
4. Plastic-window patterns provided additional information regarding gas-flow paths and qualitative indications of surface-temperature variations.
5. The ratio of the combustion temperature to the molecular weight of the products, calculated from gas velocities obtained from the combustion photographs, was computed to be 40 to 70 percent of the theoretical value.
6. Variation of ignition delay from improper mixing indicates a propellant mixture ratio that can cause starting explosions, midrun explosions, and other short-duration transient phenomena.
7. Low-frequency oscillations of approximately 100 cycles per second were recorded during some runs. Some of the starts gave frequencies of 100 to 300 cycles per second.
8. Combustion-chamber oscillations were recorded that

approximately corresponded to the resonant frequencies of the length and thickness of the combustion chamber.

LEWIS FLIGHT PROPULSION LABORATORY,  
NATIONAL ADVISORY COMMITTEE FOR AERONAUTICS,  
CLEVELAND, OHIO, May 22, 1953.

#### REFERENCES

1. Altseimer, John H.: Photographic Techniques Applied to Combustion Studies—Two-Dimensional Transparent Thrust Chamber. *Jour. Am. Rocket Soc.*, vol. 22, no. 2, Mar.-Apr. 1952, pp. 86-91.
2. Berman, Kurt, and Logan, Stanley E.: Combustion Studies with a Rocket Motor Having a Full-Length Observation Window. *Jour. Am. Rocket Soc.*, vol. 22, no. 2, Mar.-Apr. 1952, pp. 78-85.
3. Berman, Kurt, and Cheney, Samuel H., Jr.: Combustion Studies in Rocket Motors. *Jour. Am. Rocket Soc.*, vol. 23, no. 2, Mar.-Apr. 1953, pp. 89-95; discussion, pp. 96-98.
4. Tischler, Adelbert O., and Bellman, Donald R.: Combustion Instability in an Acid-Heptane Rocket with a Pressurized-Gas Propellant Pumping System. NACA TN 2936, 1953. (Supersedes NACA RM E51G11.)